A subset of dysregulated metabolic and survival genes is associated with severity of hepatic steatosis in obese Zucker rats[S]

Xabier Buqué,* María José Martínez,* Ainara Cano,* María E. Miquilena-Colina,[†,§] Carmelo García-Monzón,[†,§] Patricia Aspichueta,[1,*] and Begoña Ochoa[1,2,*]

Department of Physiology,* University of the Basque Country Medical School, Bilbao, Spain; Liver Research Unit,[†] Centro de Investigación Biomédica en Red de Enfermedades Hepáticas y Digestivas,[§] University Hospital Santa Cristina, Madrid, Spain

Abstract **We aimed to characterize the primary abnormalities associated with fat accumulation and vulnerability to hepatocellular injury of obesity-related fatty liver. We performed functional analyses and comparative transcriptomics of isolated primary hepatocytes from livers of obese insulin-resistant Zucker rats (comprising mild to severe hepatic steatosis) and age-matched lean littermates, searching for novel genes linked to chronic hepatic steatosis. Of the tested genome, 1.6% was identified as steatosis linked. Overexpressed genes were mainly dedicated to primary metabolism (100%), signaling, and defense/acute phase (~70%); detoxification, steroid, and sulfur metabolism (~65%) as well as cell growth/proliferation and protein synthesis/transformation (~70%) genes were downregulated. The overexpression of key genes involved in de novo lipogenesis, fatty acid and glycerolipid import and synthesis, as well as acetyl-CoA and cofactor provision was paralleled by enhanced hepatic lipogenesis and production of large triacylglycerol-rich VLDL. Greatest changes in gene expression were seen in those encoding the lipogenic malic enzyme (up to 7-fold increased) and cell-to-cell interacting cadherin 17 (up to 8-fold decreased). Among validated genes, fatty acid synthase, stearoyl-CoA desaturase 1, fatty acid translocase/Cd36, malic enzyme, cholesterol-7α hydroxylase, cadherin 17, and peroxisome proliferator-activated receptor α significantly correlated with severity of hepatic steatosis. In conclusion, dysregulated expression of metabolic and survival genes accompany hepatic steatosis in obese insulin-resistant rats and may render steatotic hepatocytes more vulnerable to cell injury in progressive nonalcoholic fatty liver disease.**—Buqué, X., M. J. Martínez, A. Cano, M. E. Miquilena-Colina, C. García-Monzón, P. Aspichueta, and B. Ochoa. **A subset of dysregulated metabolic and survival genes is associated with severity of hepatic steatosis in obese Zucker rats.** ***J. Lipid Res.*** **2010.** 51: **500–513.**

Supplementary key words gene expression • lipid synthesis • triglyceride secretion

An excessive accumulation of triglycerides (TGs) and cholesterol esters (ChEs) within hepatocytes is the putative "first hit" in the pathogenesis of nonalcoholic fatty liver disease (NAFLD). It encompasses a wide spectrum of hepatic pathology, ranging from simple steatosis to steatohepatitis, with progressive fibrosis and cirrhosis (1–3). The mechanisms leading to NAFLD are unclear, but its prevalence increases dramatically with obesity (4, 5) and type 2 diabetes (6). It is recognized that these two disorders are connected with fatty liver (7, 8), which has been defined as a chronic inflammatory disorder associated with endoplasmic reticulum stress (9) and mitochondrial dysfunction (10). There is also increasing evidence that NAFLD is not as benign as previously considered, but why only a minority of individuals develop progressive disease remains uncertain.

Hepatocellular TG concentrations are under stringent control by transport and catalytic proteins that facilitate the uptake of circulating NEFAs and lipoprotein esterified fatty acids, de novo FA synthesis and esterification (input), as well as cellular FA oxidation and TG export as VLDL (output) (11). Endocrine and metabolic mediators derived from the peripheral insulin action modulate the hepatocyte function. Insulin does not suppress adipose tissue lipoly-

This study was supported by grants from the Ministerio de Educación y Ciencia (SAF2007/60211), the Instituto de Salud Carlos III (RETIC G03/015 and PI06/0221), and Gobierno Vasco (Saiotek calls and IT-325-07). CIBERehd is funded by the Instituto de Salud Carlos III, Spain.

Manuscript received 6 September 2009 and in revised form 24 September 2009.

Published, JLR Papers in Press, September 24, 2009
DOI 10.1194/jlr.M001966

Abbreviations: ACC, acetyl-CoA carboxylase; apo, apolipoprotein; ChE, cholesterol ester; HOMA, homeostasis model assessment; IR, insulin resistance; NAFLD, nonalcoholic fatty liver disease; NASH, nonalcoholic steatohepatitis; PPAR, peroxisome proliferator-activated receptor; qPCR, quantitative real-time polymerase chain reaction; SREBP, sterol-regulatory element binding protein; TG, triglyceride; ZL, Zucker lean; ZO, Zucker obese.

[1] Senior co-author.
[2] To whom correspondence should be addressed.
e-mail: begona.ochoa@ehu.es

[S] The online version of this article (available at http://www.jlr.org) contains supplementary data in the form of one table.

sis nor activate LPL to the same extent in insulin-resistant states as it does in healthy patients (12, 13). Hence, hepatic fat accumulation occurs when increased delivery of NEFA and TG-rich lipoproteins accompanies increased hepatic FA synthesis (14). NAFLD is also associated with hypertriglyceridemia, mainly from the overproduction of large, TG-rich VLDL (15). This effect may be due, in part, by hepatic insulin resistance (IR) (16), but the mechanisms involved are not completely understood, and a more comprehensive examination of the fat-insulted hepatocyte is desirable.

Although recent findings implicate enhanced mitochondrial cholesterol content in the development of nonalcoholic steatohepatitis (NASH) (17), dysregulation of ChE homeostasis in fatty liver is much less understood. In this regard, hepatocyte ChE metabolism is driven by bile acid demand, transport, and catalytic proteins that facilitate lipoprotein uptake, cholesterol synthesis, and esterification with a long-chain FA (input) as well as ChE hydrolysis and export as VLDL (output). Upstream, complex integrated networks of proteolysis- or ligand-activated transcription factors play critical roles in maintaining fuel and FA and sterol lipid homeostasis (18, 19).

Molecular information on NAFLD would be biased if the total liver is examined, as the hepatocytes account for ~80% of liver volume, while nonparenchymal cells make up ~40% of the total cellularity. Similar inaccuracies would occur if only a liver biopsy sample is examined, as it represents ~1:50,000 of total liver mass. To overcome these potential pitfalls, we identified transcriptomic abnormalities in isolated primary hepatocytes from obese Zucker rats and their lean littermate controls. Obese, insulin-resistant Zucker rats develop early hepatic steatosis but do not spontaneously progress to steatohepatitis (20), thus providing a good model for the study of mechanisms underlying the "first hit." An additional aim of this work was to identify novel genes that may explain why fatty livers are more vulnerable to a challenging "second hit." We have identified a set of 108 genes that discriminates hepatocytes from mild-to-severe steatotic livers from controls and have observed that early activation of the lipogenic program, lipogenesis, and TG-rich VLDL export occurs in-tandem with downregulation of tissue structure, steroid metabolism, detoxification, and cell growth and proliferation genes. Our results strongly support the concept that aberrations in the steatotic hepatocyte extend beyond lipid accumulation.

MATERIALS AND METHODS

Animals

Animal procedures were approved by the University of the Basque Country Ethical Committee. Male Zucker *fa/fa* obese rats of 6, 9, and 12 weeks of age (ZO6, ZO9, and ZO12: 12, 12, and 16 rats, respectively) and age-matched lean controls (ZL6, ZL9, and ZL12: 12, 12, and 16 rats, respectively) were used (Charles River, Barcelona, Spain). Separate animal subgroups (n = 4–8/subgroup) were used for liver morphology and lipid analysis; gene expression profiling and lipogenesis analysis; and hepatic lipoprotein production. Animals were fed ad libitum normal maintenance diet containing 15.8% protein, 3.1% lipid, and 60.1% carbohydrate, of which 44.4% is starch and 2.3% total sugars (Panlab D04 diet; Panlab, Cornella, Spain). On the morning the rats were euthanized, they were food deprived for 1 h before being anesthetized (60 mg/kg sodium pentobarbital, ip) and euthanized.

Liver sampling and serum biochemistry

Blood was collected from the inferior cava vein; serum was used for routine biochemistry. In addition, serum insulin (Diagnostic Products, Los Angeles, CA) and leptin (Linco Research, St. Charles, MO) concentrations were determined by ELISA. Insulin resistance was calculated by the homeostasis model assessment (HOMA) index (21). Livers were quickly removed, weighed, and used for histology and lipid analysis.

Liver histology and lipid quantification

Formalin-fixed, paraffin-embedded liver sections (5 μm thick) were stained with hematoxylin and eosin and examined by an experienced pathologist blinded to the animal groups. Hepatic steatosis was defined as the percentage of hepatocytes containing macrovesicular fat droplets. The steatosis degree was evaluated in 10 randomly chosen fields (20× magnification) from each liver specimen and graded as follows: grade 0 (<5% of hepatocytes affected), grade 1 (5–32% of hepatocytes affected), grade 2 (33–66% of hepatocytes affected), or grade 3 (>66% of hepatocytes affected). For lipid quantification, livers (0.5 g) were homogenized in 10 mM PBS (4 ml), lipids were exhaustively extracted from homogenates, and lipid classes quantified as detailed elsewhere (22).

Isolation of hepatocytes and cellular RNA

Rat hepatocytes were isolated as previously described (23) and used immediately for transcriptomics or functional studies. The hepatocyte suspensions had >80% viability and were >99% nonparenchymal cell free. Total RNA was extracted from 10×10^6 hepatocytes using TRIzol (Invitrogen, Carlsbad, CA) purified (RNeasy kit; Qiagen, Hilden, Germany), DNase I treated (Invitrogen, Carlsbad, CA), and repurified according to the manufacturers' instructions. The integrity, purity, and quantity of RNA were assessed as recommended by Affymetrix (Santa Clara, CA).

Microarray hybridization and data mining

Gene expression analysis was performed by Progenika Biopharma (Derio, Spain) using the Affymetrix GeneChip® Rat Genome U34A Set and platform. Equal RNA amounts from each hepatocyte isolation from four animals of the same subgroup were pooled and used to synthesize cDNA (Invitrogen). Three independent cDNAs were generated, which were used for both microarray and quantitative PCR analyses. Biotinylated cRNAs were transcribed from cDNA templates and handled with strict adherence to the labeling, fragmentation, and hybridization protocols provided by Affymetrix. Signal and change calls were computed with statistical algorithms included in Affymetrix MAS 5.0 software and the parametric Welch *t*-test (GeneSpring; Silicon Genetics, Redwood City, CA). Files including a further description of the methodology, according to MIAME guidelines, and average differences and detection call values for all 24,000 sequences on chips are deposited in ArrayExpress repository under accession number E-MEXP-1414.

The functional profiles of extracted genes were analyzed by the NetAffx™ Analysis Center (http://www.netaffx.com/),

Panther Classification System (24) (www.pantherdb.org/), and FatiGO (25) (www.fatigo.org/).

Quantitative real-time PCR

Quantitative real-time PCR (qPCR) was performed for selected genes on the three independent cDNAs generated from the pooled RNA samples used for microarrays. Quantification was performed with an ABI PRISM 7000HT using TaqMan Assay-on-Demand probes (available upon request) (Applied Biosystems, Foster City, CA). The relative quantities of each gene were determined by the $\Delta\Delta C_T$ method. Normalization was performed using the Visual Basic Application GeNorm (26). According to GeNorm, 18S rRNA and cyclophilin were suitable genes for normalization for these studies.

Determination of lipogenic enzyme activity

The cytosol of hepatocytes (30×10^6) was used to assess glucose 6-phosphate dehydrogenase (27), malic enzyme (28), and acetyl-CoA carboxylase (ACC) (29) activity. Protein was determined by Pierce reagent using BSA as standard.

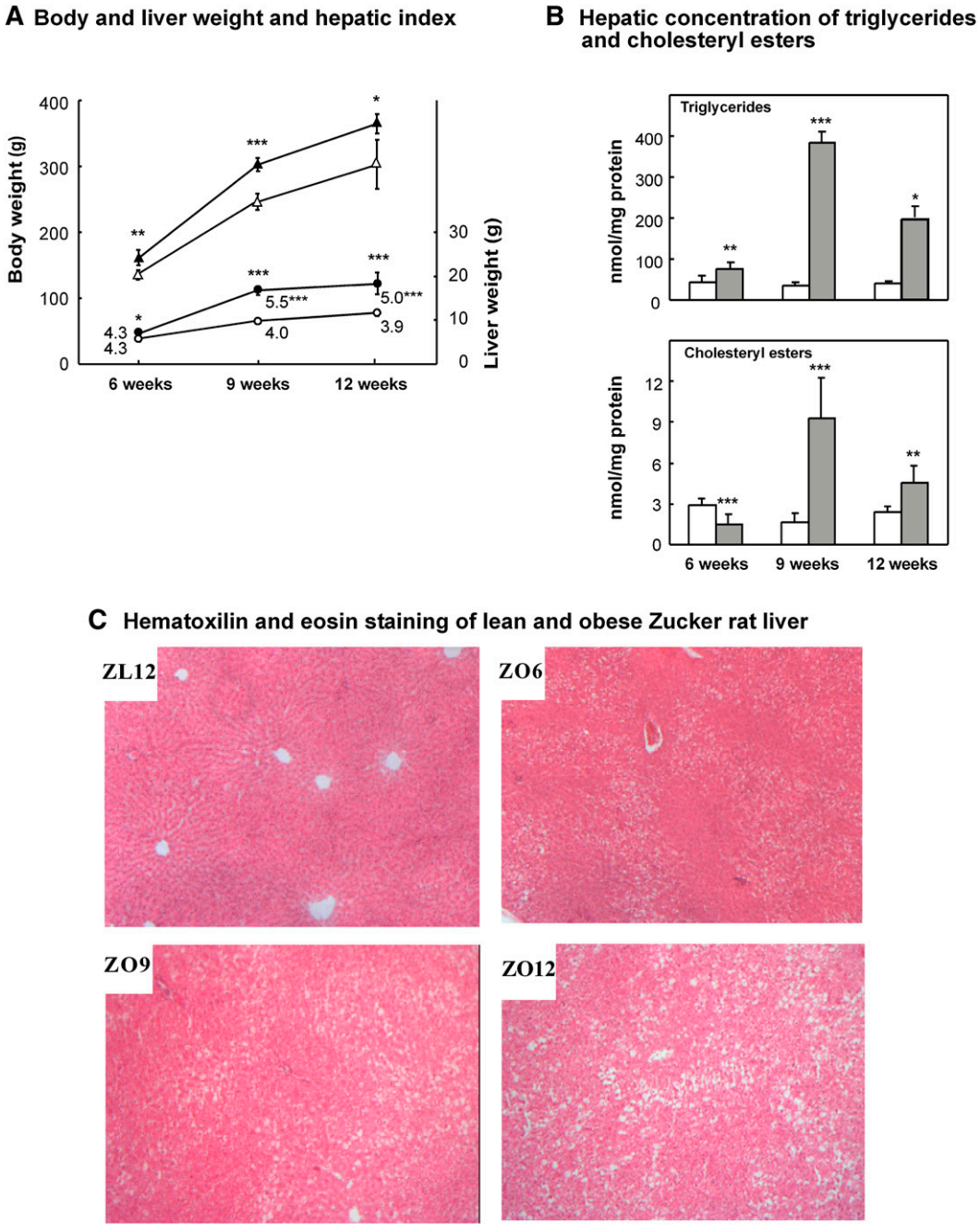

Fig. 1. Time course of hepatic steatosis in obese Zucker rats. A: Age-dependent increases of body weight (BW), liver weight (LW), and hepatic index (LW/BW in g ×100, shown in numerals). B: Hepatic concentrations of TGs and ChEs in obese Zucker rats of 6, 9, and 12 weeks (ZO6, ZO9, and ZO12; closed symbols and bars) compared with their age-matched lean controls (ZL; open symbols and bars). C: Representative H and E staining of lean (ZL12) and obese rats. Original magnification: 20× . Mean ± SD from eight (A) or four (B and C) animals; $*P < 0.05$, $**P < 0.01$, and $***P < 0.001$.

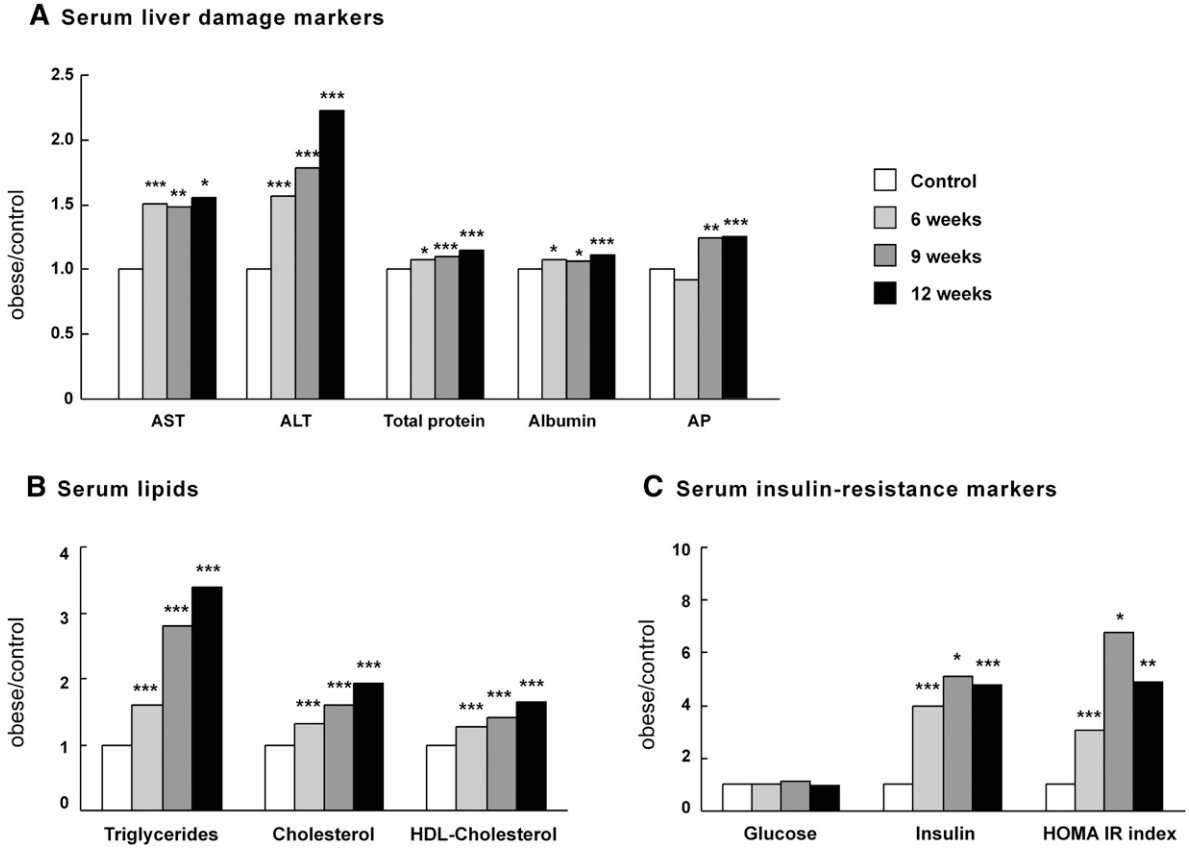

Fig. 2. Kinetic profile of serum liver damage markers, serum lipids, and serum insulin resistance markers in obese Zucker rats. Values are expressed as the ratio of concentrations in obese rats (closed bars, gray intensities explained in the inset) and the corresponding age-matched lean controls (depicted as a single open bar for each parameter). The absolute values of the three control groups are given in Table 1. Twelve (6 weeks and 12 weeks) and 16 (9 weeks) animals were used in each obese and lean group. $*P < 0.05$, $**P < 0.01$, and $***P < 0.001$.

Determination of hepatic VLDL production

After fasting for 5 h, rats were injected ip 600 mg/kg tyloxapol (Triton WR1339; Sigma-Aldrich, St. Louis, MO) to inhibit VLDL-TG hydrolysis by LPL. After 2 h, blood was collected and VLDLs (d < 1.006 g/ml) were isolated and characterized (23). The VLDL-TG and VLDL-apoB post-Triton accumulation in the serum serves as a measure of VLDL production rate. Lipoprotein sizing was estimated by light scattering (Zetasizer 4; Malvern Instruments, Malvern, UK).

Statistical analysis

Except for gene expression, results are reported as mean ± SD for the number of animals indicated. Differences between groups were assessed by the unpaired *t*-test or the Mann-Whitney *U* test, as appropriate. The Spearman's *r* test was used to evaluate correlations between mRNA levels of validated genes by qPCR, expressed as fold change compared with controls, and the percentage of steatotic hepatocytes in each group of animals studied. A $P < 0.05$ value was considered significant. All these calculations were performed using SPSS 15.0 statistical software (SPSS, Chicago, IL).

RESULTS

Hepatic steatosis, dyslipidemia, and insulin resistance in obese Zucker rats

Hepatomegaly and the hepatic index (liver weight/body weight in g, × 100) increased sharply from 6–9 weeks of age and then plateaued or decreased moderately (**Fig. 1A**). TG concentration peaked in ZO9 livers, it being 8-fold higher than ZO6 and 2-fold higher than ZO12, which in turn increased 2–4-fold over their respective controls (Fig. 1B). Concentration of cholesteryl ester also augmented in ZO9 and ZO12 livers (5- and 2-fold) but not in ZO6. Unesterified cholesterol, phospholipid, and protein concentrations were unaffected by steatosis (data not shown). Liver histology revealed variable degrees of steatosis, predominantly macrovesicular around the pericentral

TABLE 1. Blood biochemistry of control rats

Analyte[a]	6 Weeks	9 Weeks	12 Weeks
Aspartate aminotransferase (U/l)	136 ± 27[b]	119 ± 32	122 ± 34
Alanine aminotransferase (U/l)	61 ± 17	55 ± 9	49 ± 7
Protein (g/l)	50.0 ± 3.4	55.5 ± 2.3	57.7 ± 3.0
Albumin (g/l)	36.5 ± 1.9	38.7 ± 2.1	39.7 ± 1.5
Alkaline phosphatase (U/l)	335 ± 33	215 ± 33	159 ± 15
TGs (mM)	1.0 ± 0.2	0.9 ± 0.2	0.8 ± 0.2
Cholesterol (mM)	2.4 ± 0.2	2.1 ± 0.1	2.0 ± 0.2
HDL-cholesterol (mM)	1.9 ± 0.1	1.8 ± 0.1	1.7 ± 0.1
Glucose (mM)	8.3 ± 0.7	8.7 ± 1.5	9.0 ± 1.4
Insulin (mIU/l)	19.2 ± 7.0	21.9 ± 10.1	17.4 ± 6.4
HOMA-IR index	6.5 ± 1.8	8.0 ± 4.4	6.8 ± 2.4
Leptin (mg/l)	24 ± 4	31 ± 7	31 ± 10

[a] Analytes were determined as described for Fig. 2.
[b] Values are means ± SD from 12 (6 and 12 weeks) or 16 (9 weeks) animals.

zone (Fig. 1C). Grade 2 steatosis was observed in the livers of 6 (ZO6: 39 ± 4% of steatotic hepatocytes) and 9 week old Zucker rats (ZO9: 55 ± 6% of steatotic hepatocytes), whereas grade 3 steatosis was seen in the livers of 12 week old Zucker rats (ZO12: 76 ± 6% of steatotic hepatocytes). There was a significant difference in the percentage of steatotic hepatocytes between ZO12 and ZO9 rats ($P < 0.001$) as well as between ZO9 and ZO6 rats ($P = 0.001$).

Serum ALT (**Fig. 2A**), serum lipids (Fig. 2B), and serum leptin increased with body weight gain (normal values in **Table 1**). Notably, the rise in serum TG was greater than that of total cholesterol and HDL cholesterol (Fig. 2B). Leptin rose from basal concentrations (Table 1) to 273 ± 78, 293 ± 12, and 391 ± 46 mg/l in ZO6, ZO9, and ZO12, respectively. Fig. 2C shows the evolution of hyperinsulinemia and increased HOMA-IR index, both peaking at 9 weeks.

A transcriptomic view of primary hepatocytes from steatotic livers

We used Affymetrix U34AGeneChip® that contained 24,000 probe sets representing 8,799 transcripts and expressed sequence tags derived from >7,000 genes, roughly one-third of the protein coding capacity of the rat genome. A core steatosis set was defined as the genes scored as present in all groups that changed statistically ($P < 0.05$) in the same direction in the three comparisons. Hierarchical clustering of the steatosis-linked sequences was applied using GeneSpring (**Fig. 3A**). A clear-cut gene clustering of the test and control samples was achieved by both the Spearman and the Pearson correlation. Like for most phenotypic features (Figs. 1 and 2), dendograms revealed closer differential expression patterns between 9 and 12 week groups. A set of sequences (160 upregulated and 57 downregulated; Fig. 3B), encoding 108 proteins of known function, were identified as steatosis linked. PANTHER (24) scored as

A Hierarchical clustering

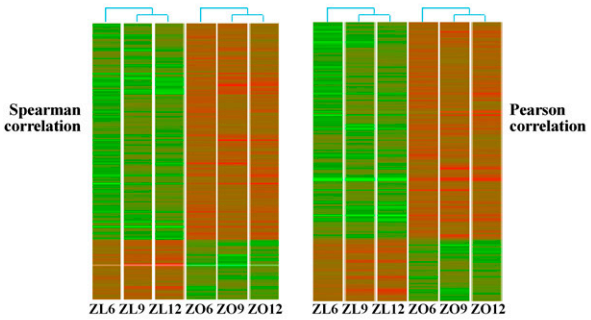

B Number of differentially expressed sequences in steatosis depicted in Venn diagrams

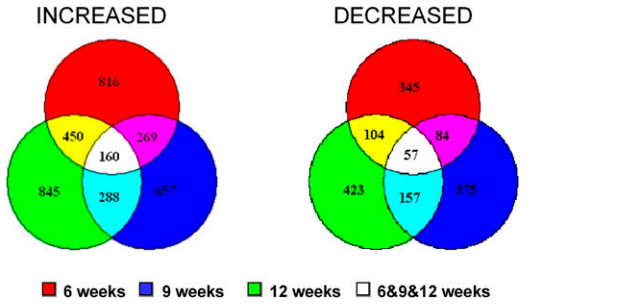

C Functional profiles of the steatosis genes set

Biological process

Significantly overexpressed	Sequences analyzed	P value
Lipid, fatty acid and steroid metabolism	343	1.86E-12
Fatty acid metabolism	97	2.07E-09
Carbohydrate metabolism	226	4.47E-09
Other carbon metabolism	29	7.69E-05
Biological process unclassified	1111	8.51E-05
Electron transport	127	1.13E-04
Pentose-phosphate shunt	2	4.26E-04
Monosaccharide metabolism	24	4.72E-04
Glycolysis	28	8.36E-04
Coenzyme and prosthetic group metabolism	76	9.60E-04
Nucleoside, nucleotide and nucleic acid metabolism	699	1.25E-03
Signal transduction	1255	1.96E-03
Fatty acid biosynthesis	17	2.14E-03
Oxidative phosphorylation	26	6.97E-03
Ion transport	294	1.13E-02
Tricarboxylic acid pathway	11	1.18E-02
Amino acid metabolism	99	1.60E-02
Cell cycle	256	2.05E-02
Developmental processes	682	2.06E-02
mRNA transcription	356	2.83E-02
Polyphosphate catabolism	2	2.92E-02
Phospholipid metabolism	45	2.96E-02
Cell structure and motility	346	3.23E-02
Significantly underexpressed		
Steroid metabolism	136	2.52E-05
Electron transport	127	1.37E-03
Other metabolism	151	1.68E-02
Signal transduction	1255	2.15E-02
Sulfur metabolism	35	2.22E-02
Stress response	92	2.23E-02
Oncogene	36	2.34E-02
Detoxification	41	2.98E-02
mRNA transcription regulation	286	3.77E-02
Induction of apoptosis	52	3.58E-02

Molecular function

Significantly overexpressed	Genes modified	P value
Acyltransferase	8	3.82E-09
Dehydrogenase	10	3.44E-07
Oxidoreductase	15	1.34E-06
Transferase	12	6.49E-05
Lyase	6	3.38E-04
Nucleic acid binding	1	2.11E-03
Acetyltransferase	3	2.87E-03
Lipase	3	4.97E-03
Decarboxylase	2	8.13E-03
Transaldolase	1	1.21E-02
Transketolase	1	1.21E-02
Synthase and Synthetase	4	1.40E-02
Phospholipase	2	2.85E-02
Carbohydrate kinase	2	3.28E-02
Phosphatase	4	3.29E-02
Significantly underexpressed		
Dehydratase	2	4.07E-03
Histone	2	4.07E-03
Oxygenase	3	8.66E-03
CREB transcription factor	1	1.56E-02
Other transferase	2	3.48E-02

Fig. 3. A global transcriptional view of steatotic hepatocytes from obese Zucker rats. A: Hierarchical clustering of differentially expressed transcripts by GeneSpring. In red, upregulated sequences, and in green, downregulated sequences; unchanged sequences have been omitted. Data in B and C are derived from differentially regulated sequences in steatosis, categorized by PANTHER. B: Venn diagrams. C: Top biological processes and molecular functions.

TABLE 2. A transcriptomic signature of obesity-related steatosis in rat hepatocytes

Accession Number	Gene Symbol	Unigene Title	Increase Fold 6 wk	9wk	12wk
Lipid Metabolism					
Synthesis and import of fatty acids into hepatocytes					
M76767	Fasn	Fatty acid synthase	2.5	3.2	5.3
X13527		Fatty acid synthase (acyl carrier domain)	2.1	4.0	6.5
J02585	Scd1	Stearoyl-CoA desaturase I	1.4	1.5	1.4
AI175764			3.7	2.6	5.3
AF036761	Scd2	Stearoyl-CoA desaturase II	3.2	5.3	4.0
AA892832	Elovl5	Long-chain fatty acid elongase I, ELOVL, family member 5	1.6	1.7	1.5
AF072411	Cd36	CD36 antigen, fatty acid translocase	2.1	4.3	5.3
AA925752			3.7	4.0	8.1
AA946388			4.0	2.8	4.6
S69874	Fabp5	Fatty acid binding protein 5, epidermal	1.2	2.5	2.1
Provision of cytosolic NADPH and acetyl-CoA for de novo lipogenesis					
M26594	Me1	Malic enzyme	2.8	3.5	4.6
AI008020			2.3	2.5	4.9
AI171506			2.6	7.5	3.7
X07467	G6pdx	Glucose-6-phosphate dehydrogenase	2.3	3.0	3.0
BC100618	Acly	ATP-citrate lyase	2.1	1.7	3.7
Glycerolipid and lipoprotein metabolism					
U36771	Gpam	Glycerol-3P-acyltransferase mitochondrial	3.2	2.0	2.5
AA893191	Ppap2c	Phosphatidic acid phosphatase, type 2C (PAP-2C)	2.0	1.6	1.7
L12380	Arf1	ADP-ribosylation factor 1	1.5	1.5	1.2
AA859529	Dgat1	Diacylglycerol-*O*-acyltransferase 1	1.3	1.2	1.2
AA893280	Adrp	Adipose differentiation-related protein, adipophilin, EST	1.7	1.2	1.7
K01934	Thrsp	Thyroid hormone responsive protein SPOT 14 protein (S14)	1.4	1.5	3.2
D10262	Chka	Choline kinase α	2.0	1.2	1.2
AA892864	Mgll	Monoglyceride lipase	1.7	1.5	1.7
AA800220	Lypla1	Lysophospholipase 1	1.6	1.5	1.5
M16235	Lipc	Hepatic lipase	1.7	1.2	1.3
L07114	Apobec1	Apolipoprotein B editing complex 1	1.5	1.5	1.6
Mitochondrial and peroxisomal oxidation of fatty acids					
AB012933	Acsl5	Acyl-CoA synthetase long-chain family member 5	1.5	2.5	1.7
U26033	Crot	Carnitine *O*-octanoyl transferase	2.1	2.5	2.8
L07736	Cpt1a	Carnitine palmitoyl transferase 1, liver	1.6	1.6	1.1
J02749	Acaa1	Acetyl-CoA acyltransferase 1	2.5	3.2	2.8
J05029	Acadl	Long chain acetyl-CoA dehydrogenase	1.2	1.5	1.2
AI168942	Bckdhb	Branched-chain keto acid dehydrogenase E1	1.1	1.1	1.3
AI170568	Dci	Dodecenoyl-CoA delta isomerase	1.5	1.5	1.9
D00729			1.2	1.9	1.5
Carbohydrate Metabolism					
Glycogen catabolism					
M59460	Pygl	Liver glycogen phosphorylase	1.3	1.2	1.3
Fructose and glucose metabolism. Glycolysis and pentose-phosphate pathway					
D13871	Scl2a5	Solute carrier family 2, member 5 (fructose transporter)	2.8	2.8	2.8
D28562			2.1	1.7	2.0
M86235	Khk	Ketohexokinase	1.3	1.1	1.4
AA892395	Aldob	Aldolase-B	1.4	1.5	1.4
AA894296	Pgm1	Phosphoglucomutase 1	1.5	1.4	1.5
X15580	Pfkfb1	6-Phosphofructo-2-kinase/fructose-2,6-bisphosphatase 1	1.2	1.5	1.5
X02610	Eno1	Enolase 1, α	1.2	1.1	1.3
X05684	Pklr	Pyruvate kinase, liver and red blood cells	2.0	1.4	2.8
AA891800	Ppa2_predicted	Pyrophosphatase inorganic	1.9	1.4	1.5
AI059508	Tkt	Transketolase	2.0	1.3	1.6
U09256			1.4	1.2	1.5
AA799452	Taldo1	Transaldolase 1	1.7	1.1	1.6

TABLE 2. *Continued.*

Accession Number	Gene Symbol	Unigene Title	Increase Fold 6 wk	9wk	12wk
Oxidative Decarboxylation of Piruvate and Tricarboxylic Acid Cycle					
AA892828	Pdhb	Pyruvate dehydrogenase (lipoamide) β (E1 component of the pyruvate dehydrogenase complex)	3.5	2.0	2.3
D10655	Dlat	Dihydrolipoamide *S*-acetyltransferase (70 kDa mitochondrial autoantigen,	1.4	2.1	2.5
D00092		E2 component of the pyruvate dehydrogenase complex)	2.1	2.6	2.0
AA891171	Ndufc2	NADH dehydrogenase (ubiquinone) 1, subcomplex unknown, 2	1.4	1.2	1.2
AA800250	Sdha	Succinate dehydrogenase complex, subunit A, flavoprotein (Fp)	1.9	1.3	1.3
AJ223355	Slc25a10	Solute carrier family 25 (mitochondrial carrier; dicarboxylate transporter), member 10	1.4	1.3	1.4
H33101	Mcart1	Mitochondrial carrier triple repeat 1	1.3	1.2	1.3
Steroid Metabolism and Bile Secretion					
M62763	Scp2	Sterol carrier protein 2	1.6	1.4	1.5
U89280	Hsd17b9	Hydroxysteroid (17-β) dehydrogenase 9	1.4	1.4	1.5
X58294	Ca2	Carbonic anhydrase 2	1.9	1.3	1.6
AF037072	Ca3	Carbonic anhydrase 3	0.41	0.15	0.35
L15079	Abcb4	ATP-binding cassette, subfamily B (MDR/TAP), member 4	0.58	0.71	0.61
U88036	Slco1a4	Solute carrier organic anion transporter family, member 1a4	0.66	0.35	0.66
M67465	Hsd3b	Hydroxysteroid delta-isomerase, 3 β	0.57	0.76	0.81
AI105448	Hsd11b1	Hydroxysteroid 11-β dehydrogenase 1	0.50	0.57	0.66
Detoxification					
M23995	Aldh1a4	Aldehyde dehydrogenase, family 1, subfamily A4	2.1	2.1	2.3
AF001898	Aldh1a1	Aldehyde dehydrogenase, family 1, subfamily A1	1.4	1.4	2.8
AA874874	Adh4	Alcohol dehydrogenase 4 (class II), pi polypeptide	1.4	1.2	1.4
S82820	Yc2	Glutathione *S*-transferase Yc2 subunit	1.2	1.4	1.6
U73525	Txn2	Thioredoxin 2	1.2	1.1	1.4
AA924267	Cyp4a22	Cytochrome P450, family 4, subfamily a, polypeptide 22	1.3	2.8	1.9
M57718			2.1	2.3	1.6
X07259			1.4	2.0	1.9
AA852004	Glul	Glutamate-ammonia ligase (glutamine synthase)	0.71	0.61	0.76
M84719	Fmo1	Flavin-containing monooxygenase 1	0.38	0.27	0.29
X62086	Cyp3a1	Cytochrome P450, family 3, subfamily a, polypeptide 1	0.47	0.41	0.41
D38381	Cyp3a18	Cytochrome P450, family 3, subfamily a, polypeptide 18	0.27	0.41	0.53
M13646	Cyp3a11	Cytochrome P450, family 3, subfamily a, polypeptide 11	0.53	0.43	0.43
M26127	Cyp1a2	Cytochrome P450, family 1, subfamily a, polypeptide 2	0.53	0.61	0.57
L22339	Sult1c1	Sulfotransferase family, cytosolic, 1C, member 1	0.57	0.61	0.50
AA926193	Sult1c2	Sulfotransferase family, cytosolic, 1C, member 2	0.35	0.43	0.21
X65296	Ces3	Carboxylesterase 3	0.47	0.27	0.35
D00362	Es2	Esterase 2	0.62	0.41	0.43
M20629			0.66	0.41	0.43
AI102562	Mt1a	Metallothionein 1a	0.57	0.53	0.42
M11794			0.50	0.61	0.29
X57999	Dio1	Deiodinase, iodothyronine, type 1	0.66	0.43	0.43
AI639418			0.57	0.53	0.71
Cell Communication, Signal Transduction and Defense					
L19180	Ptrpd	Protein tyrosine phosphatase, receptor type, D	4.0	3.7	2.0
M74152	Prlr	Prolactin receptor	2.3	2.0	4.3
L48060			1.6	1.7	2.8
J05122	Bzrp	Benzodiazepine receptor (peripheral)	1.6	1.6	2.0
U53855	Ptgis	Prostaglandin I_2 (prostacyclin) synthase	1.6	3.0	4.0
M83143	Siat1	Sialyltransferase 1	1.9	1.5	1.7
AA800005	Cd151	CD151 antigen	1.7	1.3	1.7
AA875253	Arl1	ADP-ribosylation factor-like 1	1.5	1.5	1.2
M75153	Rab11a	RAB11a, member RAS oncogene family	2.0	1.1	1.3
X82396	Ctsb	Cathepsin B	1.5	1.4	1.3
AF089825	Inhbe	Inhibin β E	1.7	1.6	2.0
V01216	Orm1	Orosomucoid 1 (α1-acid glycoprotein)	1.4	1.5	2.0
AA891422	Hig1	Hypoxia induced gene 1	1.2	1.4	1.4
AI178135	C1qbp	Complement component 1, Q subcomponent binding protein	1.2	1.3	1.3
X78997	Cdh17	Cadherin 17	0.45	0.11	0.20
M55532	Clec4f	C-Type lectin domain family 4, member f	0.71	0.57	0.81
J00738	Obp3	Alpha-2u globulin PGCL4	0.50	0.33	0.38
L00094	Agt	Angiotensinogen	0.66	0.71	0.66
S85184	Ctsl	Cathepsin L	0.70	0.70	0.60
AI76658	Hspb1	Heat shock 27 kDa protein 1	0.57	0.57	0.27

TABLE 2. *Continued.*

Accession Number	Gene Symbol	Unigene Title	Increase Fold 6 wk	9wk	12wk
Cell Growth and Proliferation					
AA800243	Cidea_predicted	Cell-death-inducing DNA fragmentation factor, α subunit-like factor like effector A	2.6	2.5	3.0
AA893235	Gos2	G0/G1 switch protein 2	2.0	1.3	1.7
AF014503	Nupr1	Nuclear protein 1	1.5	1.9	1.7
AA891591	Pdcd8	Programmed cell death 8 (apoptosis-inducing factor)	1.3	1.3	1.4
X06150	Gnmt	Glycine *N*-methyltransferase	0.61	0.61	0.76
U17254	Nr4a1	Nuclear receptor subfamily 4, group A, member 1	0.43	0.47	0.31
Y00396	Myc	Myc viral oncogene homolog	0.71	0.47	0.23
X17163	Jun	Jun oncogene	0.66	0.71	0.47
M63282	Atf3	Activating transcription factor 3	0.53	0.66	0.47
AF020618	Myd116	Myeloid differentiation primary response gene 116	0.61	0.66	0.41
L32591	Gadd45a	Growth arrest and DNA-damage-inducible 45 α	0.71	0.57	0.33
AI176662	Egr1	Early growth response 1, nerve growth factor induced factor A	0.76	0.57	0.47
AF023087			0.71	0.66	0.57
AI177503	H3f3b	H3 histone, family 3B	0.71	0.71	0.57
Protein Synthesis and Transformation					
D13907	Pmpcb	Mitochondrial processing peptidase β	1.6	1.4	1.5
L14684	Gfm	G elongation factor (EFG)	1.2	1.2	1.4
X15096	Arbp	Acidic ribosomal phosphoprotein P0	0.43	0.76	0.76
X55153	Rplp2	Ribosomal protein P2	0.61	0.76	0.61
X59051	Rps29	Ribosomal protein S29	0.76	0.76	0.66
X14181	Mgc72957	Ribosomal protein L18a	0.76	0.76	0.76

upregulated at the $P < 0.01$ level most primary metabolic processes and at $P < 0.05$ signal transduction, cell cycle, and mRNA transcription. In contrast, steroid metabolism and trans-sulfuration pathways, detoxification, electron transport, induction of apoptosis,and mRNA transcription regulation were scored as downregulated (Fig. 3C, left). Transfer enzymes of one to three carbons, acyl fragments, phosphoryl groups, or electrons, and DNA binding proteins are primary targets of steatosis (Fig. 3C, right).

Table 2 shows the list of 108 genes categorized by our own GO-based criterion. Two categories, metabolism and detoxification, account for near 65% of the steatosis gene set. Genes with direct roles in lipid metabolism comprise 24% of the steatosis set and 36% of the upregulated group. Seventeen percent correspond to aerobic and anaerobic carbohydrate catabolism genes, all of which are upregulated. In contrast, steroid metabolism and detoxification genes make up 47% of the set whose expression is suppressed in steatosis. Most cellular communication genes (70%) are upregulated, whereas the gene subsets for defense, cell growth, and proliferation, and protein synthesis and transformation are mostly (67–69%) downregulated.

Transcriptomic and functional metabolic dysregulation in hepatocytes from steatotic livers

All (>40) direct effectors of lipid and carbohydrate metabolism genes showed significant increases in expression in steatotic hepatocytes. Critical genes for fatty acid uptake, de novo synthesis, activation and oxidation, as well as for glycerolipid synthesis were 2- to 7-fold upregulated compared with controls. These include Me1, G6pdx, and Acly, which provide NADPH and acetyl-CoA for lipogenesis, and Fasn, Elovl5, Scd1, and Scd2, which form mainly oleate and palmitoleate from saturated fatty acids, a conversion that facilitates the synthesis of storage lipids. Likewise, Cd36 that facilitates FA entry into hepatocytes showed a robust upregulation, while Lipc overexpression suggests efficient lipolytic clearance of chylomicron remnants and intermediate-density lipoprotein TG at the liver endothelium. Essential genes that handle excessive fatty acids through glycerolipid synthesis (Gpam, Ppap2c, Arf1, and Dgat1), as well as the lipid droplet formation-linked adipophilin and spot 14, were upregulated, as were critical genes involved in mitochondrial and peroxisomal fatty acid oxidation (Acsl5, Crot, Cpt1a, and Acaa1). Interestingly, expression of transcriptional regulators sterol-regulatory element binding protein 1c (SREBP1c), hepatocyte nuclear factor 4α, peroxisome proliferator-activated receptor α (PPARα), and PPARγ, however, were unaffected. In most cases, their mRNA levels in hepatocytes from low-graded steatotic livers (ZO6, with 39 ± 4% of steatotic hepatocytes) did not differ significantly from controls, while they increased sharply in hepatocytes from livers affected by severe steatosis (from 55 ± 6% to 76 ± 6% of steatotic hepatocytes) (see supplementary Table I). Particularly, SREBP1c and PPARγ transcript overexpression was documented in ob/ob and db/db mice (30) and in Zucker diabetic rats (31), all at 10–12 weeks. Work by us using qPCR showed SREBP1c mRNA overexpression in hepatocytes from Zucker fa/fa rats of 12 weeks of age but not in cells from ZO6 or ZO9 rats (data not shown). Similar findings were reported recently in 12 week old ob/ob mice and fa/fa rat livers (32), suggesting that the overexpression of SREBP1c mRNA is linked to late stages of steatosis in such murine models. Strain- and species-specific mechanisms seem to operate, moreover, in the PPARγ mRNA expression regulation, given the lack of change found by us and by Oana et al. (33) in fa/fa rats of any age.

Overexpression of genes required for fructose transport (Slc2a5), activation (Khk), and excision (Aldob); regulation of glycolysis (Pklr and Pfkfb1); and the pentose-phosphate pathway (G6pdx, Tkt, and Taldo1) were robust. Likewise, expression of two components of the pyruvate dehydrogenase complex, including the 70 kDa mitochondrial autoantigen, increased more than 2-fold. It is interesting to note that the enhanced conversion of pyruvate to acetyl-CoA within mitochondria not only supplies 2C fragments for lipogenic purposes but also for ATP production. Evaluation of glucose 6-phosphate dehydrogenase, malic enzyme, and ACC activity confirmed that such upregulated lipogenic program was effectively translated into a higher fatty acid biosynthetic activity (**Fig. 4A**), with increases of ~4–5-fold over controls recorded in hepatocytes from ZO6 and ZO9 rats and to a lesser extent in ZO12 cells.

Genes relative to VLDL assembly and cholesterol homeostasis were minimally affected. Notwithstanding, more and larger TG-rich VLDL particles were secreted by the liver of 9 week old obese rats (Fig. 4B). Estimation of the 2 h hepatic production of apolipoprotein B (apoB) and lipid in VLDL by in vivo Triton WR1339 studies revealed enhanced output of TGs by ~3-fold and of cholesterol and apoB (mostly the edited form apoB48) by ~60–100% in obese compared with lean rats. Further dynamic scattering and lipid analyses of lipoprotein particles after their chromatographic separation confirmed the presence of large TG-rich VLDLs in the circulation (Fig. 4C).

Nonmetabolic genes are markedly altered in hepatocytes from steatotic livers

Impaired detoxification and mild oxidative stress may be envisaged from the number of related genes that are downregulated in steatotic hepatocytes. Of note is the low expression of the ammonia detoxifying Glul and of a substantial number of drug-metabolizing and cytochrome genes, although the oxidative stress marker Cyp2E1 is unaffected in early steatosis. Sult1c1 and Sult1c2, encoding phase II sulfotransferases, and Slco1a4, encoding the phase III transporter organic anion transporter 1a4, as well as Gnmt, a gene necessary for glutathione synthesis, were downregulated.

As expected, steatotic hepatocytes overexpressed several cell communication and defense genes, including the inflammation-related Ptgis, the immunomodulatory Ctsb and Prlr, and acute-phase Orm1, Inhbe, and Hig1.

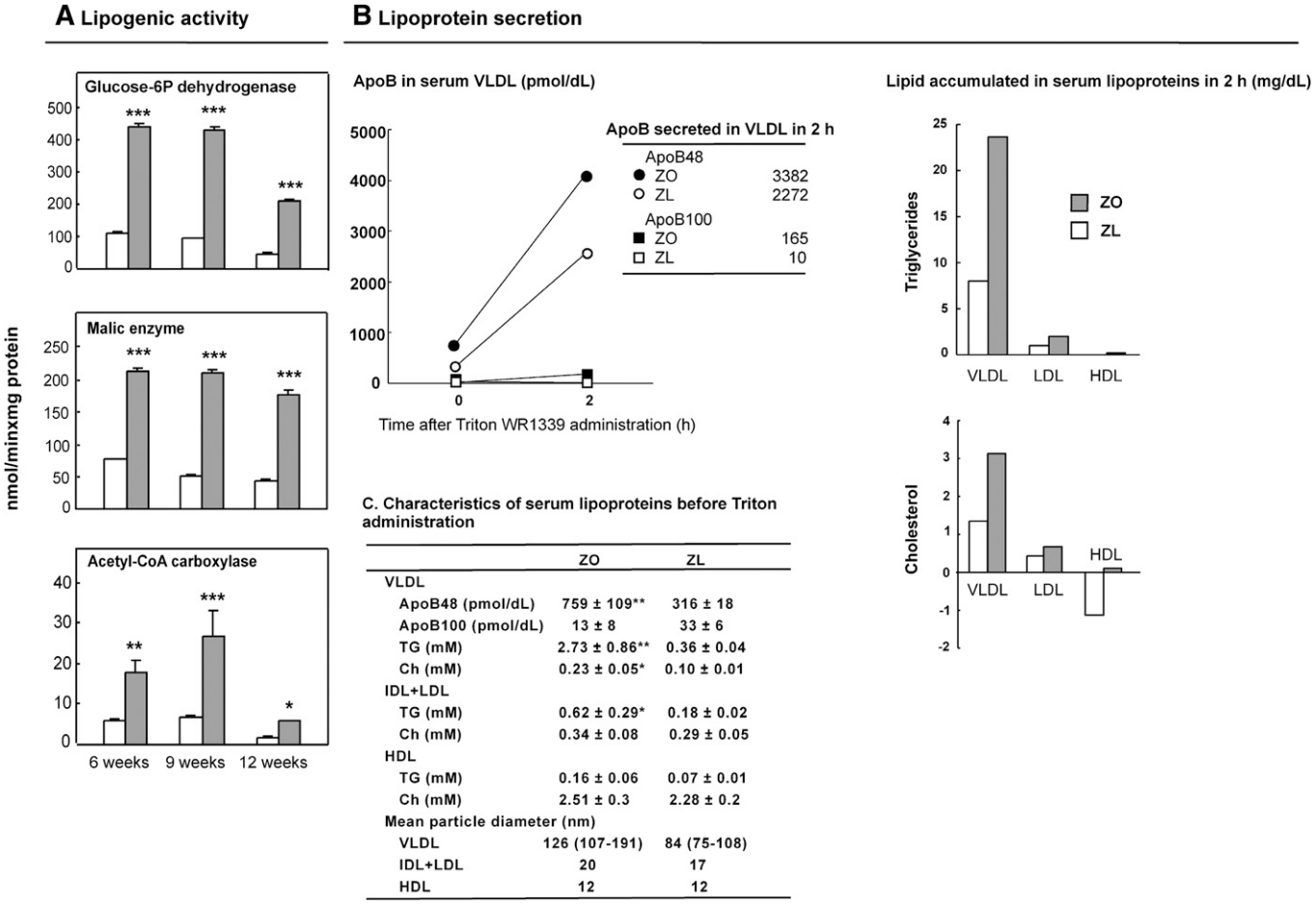

C. Characteristics of serum lipoproteins before Triton administration

	ZO	ZL
VLDL		
ApoB48 (pmol/dL)	759 ± 109**	316 ± 18
ApoB100 (pmol/dL)	13 ± 8	33 ± 6
TG (mM)	2.73 ± 0.86**	0.36 ± 0.04
Ch (mM)	0.23 ± 0.05*	0.10 ± 0.01
IDL+LDL		
TG (mM)	0.62 ± 0.29*	0.18 ± 0.02
Ch (mM)	0.34 ± 0.08	0.29 ± 0.05
HDL		
TG (mM)	0.16 ± 0.06	0.07 ± 0.01
Ch (mM)	2.51 ± 0.3	2.28 ± 0.2
Mean particle diameter (nm)		
VLDL	126 (107-191)	84 (75-108)
IDL+LDL	20	17
HDL	12	12

Fig. 4. Increased hepatic lipogenic activity and TG-rich VLDL production in obese Zucker rats. A: Glucose-6-phosphate dehydrogenase, malic enzyme, and ACC activity in hepatocytes of 6, 9, and 12 week old obese Zucker rats (ZO, closed bars) and their age-matched lean controls (ZL, open bars). B: Rats (9 weeks) were injected with 600 mg/kg Triton WR1339 or saline, blood samples were drawn before (0 h) and 2 h after injection, and lipoprotein isolated and assayed for TG and cholesterol (Ch). Lipoprotein sizing was performed in 0 h samples. Mean ± SD from four animals. $*P < 0.05$, $**P < 0.01$, and $***P < 0.001$.

In contrast, expression of cadherin 17 (up to 8-fold decreased), which is involved in tissue structure and cell-to-cell communication, was downregulated, giving a novel morphological clue for the high susceptibility of steatotic hepatocytes to injury. Some apoptosis and mitosis genes were upregulated, but others, such as c-Myc and Jun, were repressed.

The microarray data were validated by qPCR analysis of six steatosis-induced genes: Cd36, Me1, Fasn, Scd1, Acaa1, and Acsl5; two suppressed genes: Cdh17 and Egr1; and three unaffected genes: Cyp7a1, rate-limiting of bile acid synthesis; Prkaa2, the cell energy status sensor AMP kinase β_1 catalytic subunit, and the transcription factor Ppara. Although the fold change for all genes differed slightly with respect to microarrays (Table 2), the patterns of change were similar (**Fig. 5**). Fasn was the most upregulated gene (up to 11-fold increased), while Cdh17 was most downregulated (up to 8-fold decreased).

Dysregulated genes in isolated hepatocytes correlated with the histological degree of hepatic steatosis

To determine whether the dysregulation of certain genes is associated with the hepatic steatosis in obese Zucker rats, we carried out a correlation analysis between changes in hepatocyte mRNA levels of genes quantified by qPCR and the percentage of steatotic hepatocytes in each group of animals. We found that Fasn, Scd1, Cd36, and Me1 overexpression significantly correlated with severity of hepatic steatosis (Fasn, $r = 0.950$, $P < 0.001$; Scd1, $r = 0.867$, $P = 0.002$; Cd36, $r = 0.833$, $P = 0.005$; Me1, $r = 0.767$, $P = 0.015$). No statistically significant correlation was observed for Acaa1 and Acsl5 ($r = 0.477$, $P = 0.194$; and $r = 0.583$, $P = 0.099$, respectively). Among downregulated genes, Cdh17, Cyp7a1, and Ppara (the two latter not steatosis-linked by microarrays), significantly correlated with the percentage of steatotic hepatocytes (Cyp7a1, $r = 0.867$, $P = 0.002$; Cdh17, $r = 0.695$, $P = 0.037$; Ppara, $r = 0.669$, $P = 0.048$). No statistically significant correlation was observed for Egr1 ($r = -0.460$, $P = 0.213$) and Prkaa2 ($r = 0.117$, $P = 0.765$). The most significant correlations are shown in **Fig. 6**.

DISCUSSION

The key contributions of this study are the followings: *1*) clear transcriptional upregulation of the lipogenic and not of the cholesterogenic program; *2*) confirmation of increased rates of de novo lipogenesis and VLDL-TG

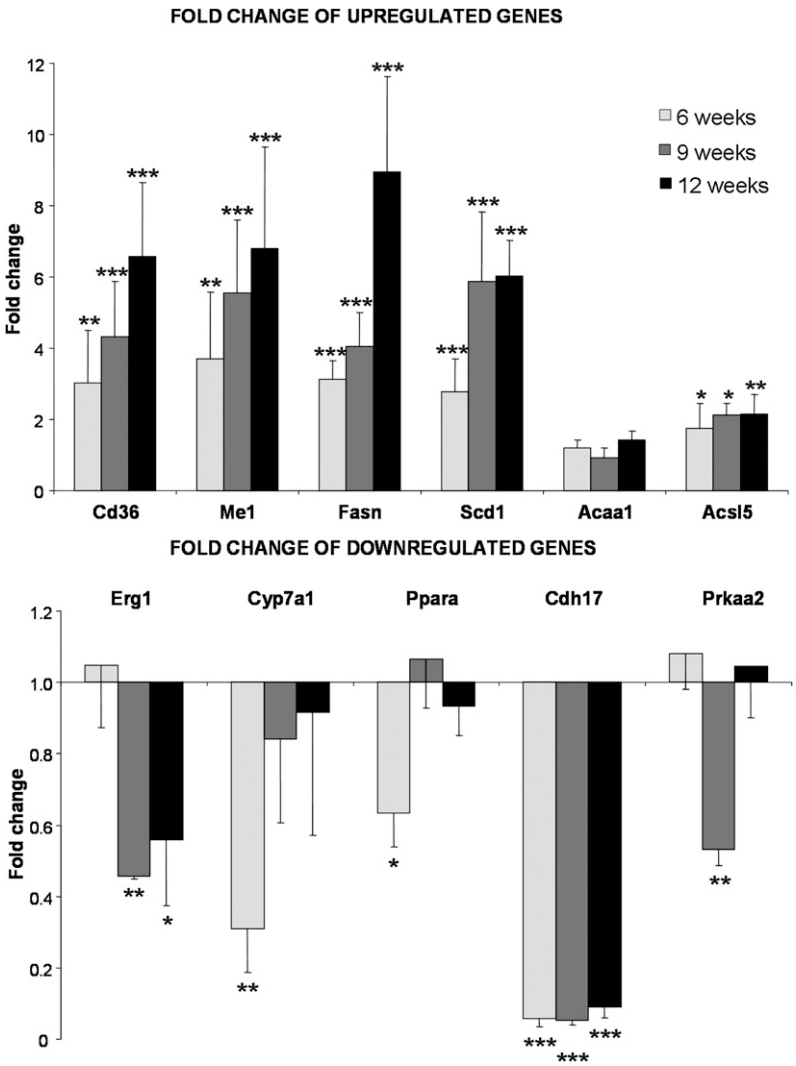

Fig. 5. Validation of microarray analysis by real-time qPCR. Expression of 11 genes was measured by qPCR in isolated hepatocytes of 6, 9, and 12 week old obese Zucker rats and their age-matched lean controls, using for normalization 18S rRNA and cyclophylin and GeNorm software. Mean ± SD from four animals. $^*P < 0.05$, $^{**}P < 0.01$, and $^{***}P < 0.001$.

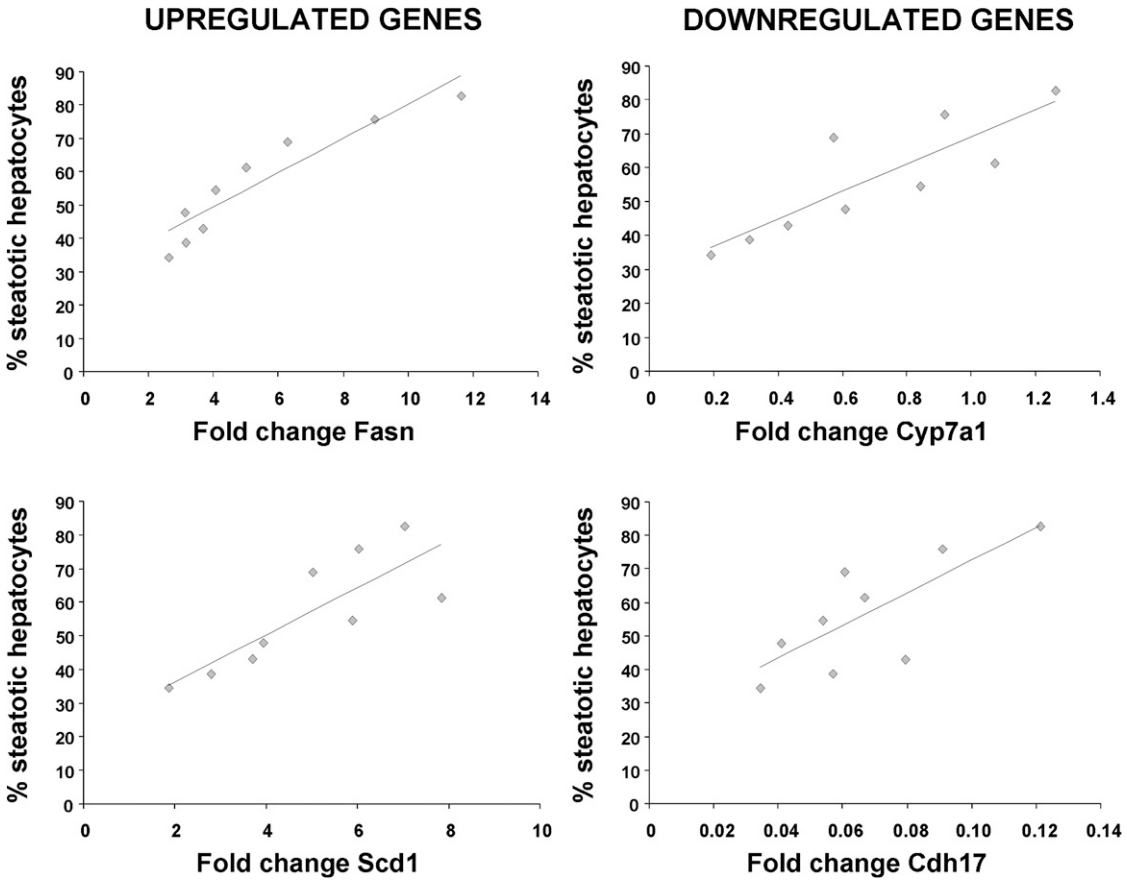

Fig. 6. Dysregulated genes in isolated hepatocytes correlated with the severity of hepatic steatosis. Significant correlations between several upregulated (left panels) and downregulated (right panels) genes and the percentage of steatotic hepatocytes in obese Zucker rats are graphically depicted. The points shown represent mean values of each age-matched group of rats. Fasn, $r = 0.950$, $P < 0.001$; Scd1, $r = 0.867$, $P = 0.002$; Cyp7a1, $r = 0.867$, $P = 0.002$; Cdh17, $r = 0.695$, $P = 0.037$

synthesis and secretion with hepatic IR; *3*) significant correlation of Fasn, Scd1, Cd36, and Me1 overexpression with severity of hepatic stetatosis; and *4*) identification of downregulated genes involved in maintaining tissue structure, detoxification, and cell survival among steatotic hepatocytes (summarized in **Fig. 7**).

Major advances have been made in understanding the metabolic alterations leading to hepatic TG accumulation. It is well known that for VLDL synthesis, TG is mobilized from cytosolic lipid droplets by lipolysis followed by reesterification of products by diacylglycerol acyltransferase-2, and some of the resulting product is transferred to nascent apoB during the assembly of primordial apoB-containing lipoproteins in the endoplasmic reticulum (34). An alternative fate for a large proportion of the TG product is return to the cytosol in what appears to be a futile cycle that is enhanced by insulin and results in VLDL output suppression (34) and, thus, a major hepatic IR target. A distinct acyltransferase (Dgat1), modestly overexpressed herein, uses preferentially the serum NEFA pool (between 61 and 81% in the postprandial-fasting condition) for the formation of the cytosolic lipid droplet TGs (35). Our results obtained from this murine model that resembles human obesity with IR phenotype (36) strongly support that fat accumulation in hepatocytes is a consequence of the upregulated expression and activity of a number of genes involved in de novo lipogenesis (Figs. 3 and 5; Table 2), peripheral and dietary NEFA uptake (Figs. 3 and 5; Table 2), and TG synthesis (Figs. 3 and 5; Table 2) (see summary in Fig. 7).

It has been proposed that the N-terminal end of apoB acquires neutral lipid to form nucleation sites in the endoplasmic reticulum and that the number of these sites may be enhanced by increased TG synthesis (37). In this model, an increased TG supply together with less TG recycling by hepatic IR may also lead to a rise in the number of lipid-containing nucleation sites for the formation of larger TG-rich VLDL particles. The hepatic overproduction of large TG-rich VLDLs (Fig. 4) observed in obese Zucker rats strongly supports this concept and is in line with clinical reports showing overproduction of large VLDLs in human diabetes and obese insulin-resistant NAFLD patients (15). There is recent animal data suggesting that hepatic steatosis may be protective in limiting the potential lipotoxicity associated with excessive NEFA output. Despite its plausibility, further studies are required as chronic steatosis increases the vulnerability of hepatocytes to a "second hit." In support of this, we have demonstrated dysregulation of genes relevant for cell survival (i.e., detoxification, steroid metabolism, cell growth, and hepatic tissue structure genes) (Figs. 3 and 7; Table 2).

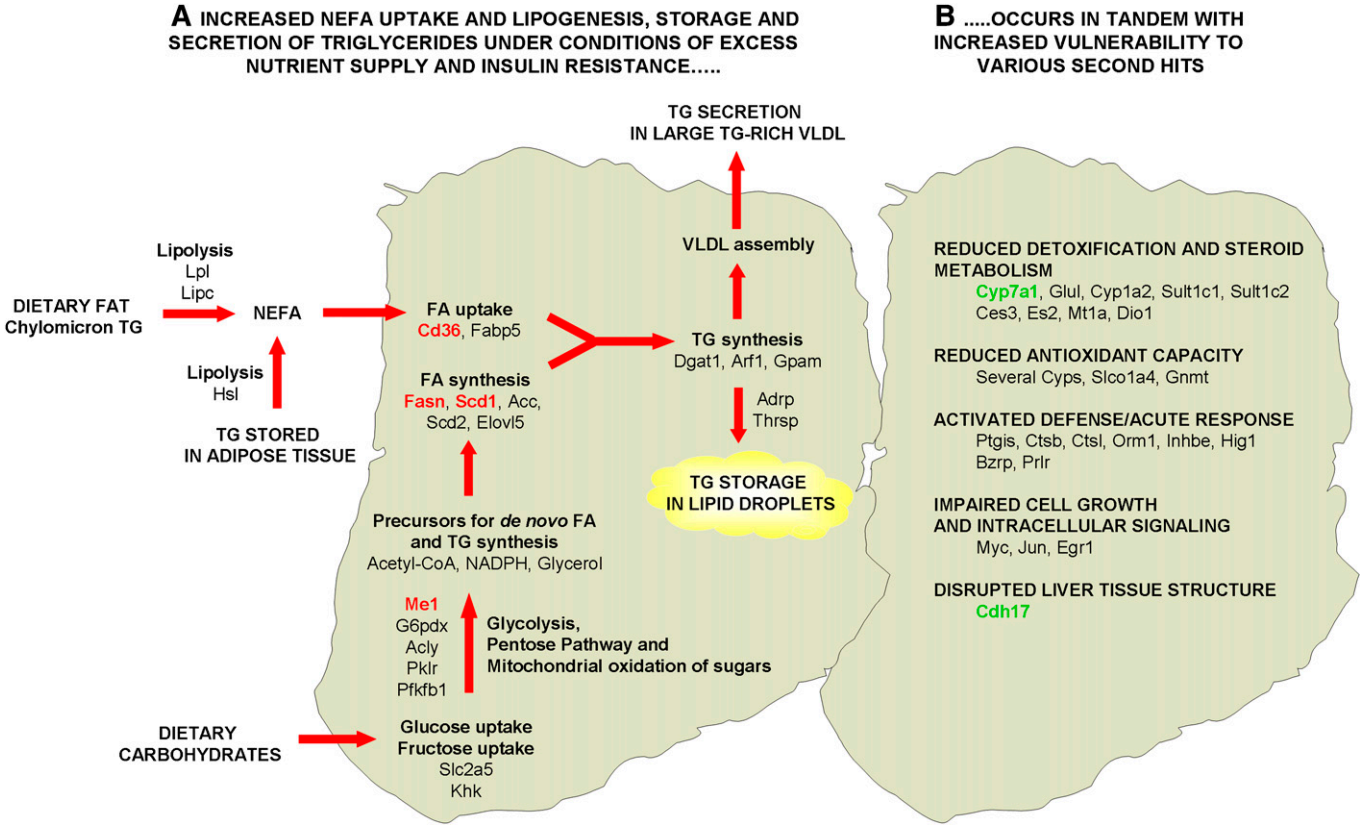

Fig. 7. In response to chronic excess nutrient supply and insulin resistance, hepatocytes become steatotic and vulnerable to various insults. A: Metabolic pathways and genes contributing to FA supply and TG accumulation in primary hepatocytes. In red: processes that are activated by microarray or functional analyses and genes whose overexpression correlates positively with steatosis severity. More than 40 direct effectors of lipid and carbohydrate metabolism genes showed significant increases in expression in steatotic hepatocytes. B: Deregulation of a panel of defense and survival genes are associated with simple steatosis. In green: genes whose repression correlates positively with steatosis severity. The unigene title for each gene is given in Table 2.

Fat accumulation in the liver is associated with decreased efficiency of the mitochondrial phosphorylative system (38). When the cells become dependent on ATP, adenylate kinase turns into action to generate ATP and AMP, whose level rises. According to a canonical line of thinking, this is sensed by AMP kinase, which switches on the ATP-producing catabolic pathways and formation of malonyl-CoA by ACC is blocked. What we have learned from the findings shown in Fig. 4 and Table 2 is that ACC is dysregulated and very active in steatotic hepatocytes and that the elevated demand of ATP for lipogenesis has to be met by glucose and fructose oxidation; the two routes appear to be transcriptionally favored. High consumption of fructose in the diet is known to cause hepatic steatosis by upregulation of lipogenic SREBPlc expression (39). A striking and novel observation is that in obesity-related hepatic steatosis, hepatocytes are predisposed for fructose uptake and oxidation in the absence of any other dietary stimuli but calorie overconsumption.

Numerous novel, steatosis-linked genes have been identified. These include Dio1 [encoding deiodinase, a selenoprotein that is downregulated in hypothyroidism, a phenotype that has been reported in patients with NASH (8, 36)] and Bzrp [encoding the peripheral-type benzodiazepine receptor that has been associated with hepatic encephalopathy due to liver failure (40)]. Additional genes (such as Me1, Scd1, Acc, Fasn, Pdhb, and Cd36) have been previously associated with liver disease (41, 42). Results in this study reinforce and extend such findings as we demonstrate for the first time that the overexpression of Me1, Cd36, Fasn, and Scd1 and the underexpression of Cdh17, Cyp7a1, and Ppara in primary hepatocytes significantly correlated with the severity of hepatic steatosis in obese rats with IR (Figs. 5 and 6), suggesting that dysregulation of these genes could play a central role in the pathogenesis of obesity-related fatty liver. The gene set associated with steatosis further includes genes encoding ligands, binding proteins, transporters, and proliferation and apoptosis regulators (Table 2). Alterations in these genes have also been identified in individuals and animal models of NASH (43), showing partial common gene signatures in human, mouse, and rat NAFLD.

In conclusion, we have identified a set of 108 genes linked to chronic hepatic steatosis in primary hepatocytes in a model of obesity and IR. We find that early activation of the complete lipogenic program, TG synthesis, and TG-rich VLDL export occurs in tandem with downregulation of tissue structure, steroid metabolism, detoxification and cell growth, and proliferation genes, indicating that gene expression abnormalities in steatotic hepatocytes are

not confined to lipid metabolism genes (Fig. 7). Further functional studies on the role of some of these steatosis-linked genes should lead to a better understanding of the early pathogenic mechanisms of hepatic steatosis and its susceptibility to liver cell damage as well as to identify molecular targets with potential therapeutic utility to modify the outcome of obesity-related fatty liver.

The authors thank M. Busto and M. Portuondo for their excellent technical assistance and E. Hilario and M.P. Portillo for their help with the interpretation of liver histology and leptin quantification.

REFERENCES

1. Angulo, P. 2002. Nonalcoholic fatty liver disease. *N. Engl. J. Med.* **346:** 1221–1231.
2. Fernández-Bermejo, M., and C. García-Monzón. 2002. A wider view on diagnostic criteria of nonalcoholic steatohepatitis. *Gastroenterology.* **122:** 840–842.
3. Adams, L. A., S. Sanderson, K. D. Lindor, and P. Angulo. 2005. The histological course of nonalcoholic fatty liver disease: a longitudinal study of 103 patients with sequential liver biopsies. *J. Hepatol.* **42:** 132–138.
4. Diehl, A. M. 1999. Nonalcoholic steatohepatitis. *Semin. Liver Dis.* **19:** 221–229.
5. Pagano, G., G. Pacini, G. Musso, R. Gambino, F. Mecca, N. Depetris, M. Cassander, E. David, P. Cavallo-Perin, and M. Rizzetto. 2002. Nonalcoholic steatohepatitis, insulin resistance, and metabolic syndrome: further evidence for an etiologic association. *Hepatology.* **35:** 367–372.
6. Gupte, P., D. Amarapurkar, S. Agal, R. Baijal, P. Kulshrestha, S. Pramanik, N. Patel, A. Madan, A. Amarapurkar, and Hafeesunnisa. 2004. Non-alcoholic steatohepatitis in type 2 diabetes mellitus. *J. Gastroenterol. Hepatol.* **19:** 854–858.
7. García-Monzón, C., E. Martín-Pérez, O. L. Iacono, M. Fernández-Bermejo, P. L. Majano, A. Apolinario, E. Larrañaga, and R. Moreno-Otero. 2000. Characterization of pathogenic and prognostic factors of nonalcoholic steatohepatitis associated with obesity. *J. Hepatol.* **33:** 716–724.
8. Lonardo, A., C. Carani, N. Carulli, and P. Loria. 2006. 'Endocrine NAFLD' a hormonocentric perspective of nonalcoholic fatty liver disease pathogenesis. *J. Hepatol.* **44:** 1196–1207.
9. Day, C. P. 2006. From fat to inflammation. *Gastroenterology.* **130:** 207–210.
10. Pessayre, D., and B. Fromenty. 2005. NASH: a mitochondrial disease. *J. Hepatol.* **42:** 928–940.
11. Musso, G., R. Gambino, and M. Cassader. 2009. Recent insights into hepatic lipid metabolism in non-alcoholic fatty liver disease (NAFLD). *Prog. Lipid Res.* **48:** 1–26.
12. Bugianesi, E., A. J. McCullough, and G. Marchesini. 2005. Insulin resistance: a metabolic pathway to chronic liver disease. *Hepatology.* **42:** 987–1000.
13. Sell, H., D. Etze-Schroeder, and J. Eckel. 2006. The adipocyte-myocyte axis in insulin resistance. *Trends Endocrinol. Metab.* **17:** 416–422.
14. Browning, J. D., and J. D. Horton. 2004. Molecular mediators of hepatic steatosis and liver injury. *J. Clin. Invest.* **114:** 147–152.
15. Adiels, M., M. R. Taskinen, C. Packard, M. J. Caslake, A. Soro-Paavonen, J. Westerbacka, S. Vehkavaara, A. Häkkinen, S. O. Olofsson, H. Yki-Järvinen, et al. 2006. Overproduction of large VLDL particles is driven by increased liver fat content in man. *Diabetologia.* **49:** 755–765.
16. Watts, G. F., and S. K. Gan. 2008. Nutrition and metabolism: non-alcoholic fatty liver disease- pathogenesis, cardiovascular risk and therapy. *Curr. Opin. Lipidol.* **19:** 92–94.
17. Mari, M., F. Caballero, A. Colell, A. Morales, J. Caballeria, A. Fernandez, C. Enrich, J. C. Fernandez-Checa, and C. García-Ruiz. 2006. Mitochondrial free cholesterol loading sensitizes to TNF- and Fas-mediated steatohepatitis. *Cell Metab.* **4:** 185–198.
18. Berger, J. P., T. E. Akiyama, and P. T. Meinke. 2005. PPARs: therapeutic targets for metabolic disease. *Trends Pharmacol. Sci.* **26:** 244–251.
19. Dentin, R., J. Girard, and C. Postic. 2005. Carbohydrate responsive element binding protein (ChREBP) and sterol regulatory element binding protein-1c (SREBP-1c): two key regulators of glucose metabolism and lipid synthesis in liver. *Biochimie.* **87:** 81–86.
20. Koteish, A., and A. M. Diehl. 2001. Animal models of steatosis. *Semin. Liver Dis.* **21:** 89–104.
21. Matthews, D. R., J. P. Hosker, A. S. Rudenski, B. A. Naylor, D. F. Treacher, and R. C. Turner. 1985. Homeostasis model assessment: insulin resistance and beta-cell function from fasting plasma glucose and insulin concentrations in man. *Diabetologia.* **28:** 412–419.
22. Ruiz, J. I., and B. Ochoa. 1997. Quantification in the subnanomolar range of phospholipids and neutral lipids by monodimensional thin-layer chromatography and image analysis. *J. Lipid Res.* **38:** 1482–1489.
23. Aspichueta, P., S. Perez, B. Ochoa, and O. Fresnedo. 2005. Endotoxin promotes preferential periportal upregulation of VLDL secretion in the rat liver. *J. Lipid Res.* **46:** 1017–1026.
24. Mi, H., N. Guo, A. Kejariwal, and P. D. Thomas. 2007. PANTHER version 6: protein sequence and function evolution data with expanded representation of biological pathways. *Nucleic Acids Res.* **35:** D247–D252.
25. Gene Ontology Consortium. 2006. The Gene Ontology (GO) project in 2006. *Nucleic Acids Res.* **34:** D322–D326.
26. Vandesompele, J., K. De Preter, F. Pattyn, B. Poppe, B., N. Van Roy, A. De Paepe, and F. Speleman, F. (2002) Accurate normalization of real-time quantitative RT-PCR data by geometric averaging of multiple internal control genes. Genome Biol. **3:** RESEARCH0034
27. Kuby, S. A., and R. N. Roy. 1976. Glucose-6-phosphate dehydrogenase from brewers' yeast. The effects of pH and temperature on the steady-state kinetic parameters of the two-chain protein species. *Biochemistry.* **15:** 1975–1987.
28. Hsu, R. Y. 1970. Mechanism of pigeon liver malic enzyme. Formation of L-lactate from L-malate, and effects of modification of protein thiol groups on malic enzyme, oxalacetate, and pyruvate reductase activities. *J. Biol. Chem.* **245:** 6675–6682.
29. Chang, H. C., I. Seidman, G. Teebor, and M. D. Lane. 1967. Liver acetyl CoA carboxylase and fatty acid synthetase: relative activities in the normal state and in hereditary obesity. *Biochem. Biophys. Res. Commun.* **28:** 682–686.
30. Memon, R. A., L. H. Tecott, K. Nonogaki, A. Beigneux, A. H. Moser, C. Grunfeld, and K. R. Feingold. 2000. Up-regulation of peroxisome proliferator-activated receptors (PPAR-alpha) and PPAR-gamma messenger ribonucleic acid expression in the liver in murine obesity: troglitazone induces expression of PPAR-gamma-responsive adipose tissue-specific genes in the liver of obese diabetic mice. *Endocrinology.* **141:** 4021–4031.
31. Alemzadeh, R., and K. Tushaus. 2005. Diazoxide attenuates insulin secretion and hepatic lipogenesis in zucker diabetic fatty rats. *Med. Sci. Monit.* **11:** BR439–BR448.
32. Kammoun, H. L., H. Chabanon, I. Hainault, S. Luquet, C. Magnan, T. Koike, P. Ferré, and F. Foufelle. 2009. GRP78 expression inhibits insulin and ER stress-induced SREBP-1c activation and reduces hepatic steatosis in mice. *J. Clin. Invest.* **119:** 1201–1215.
33. Oana, F., H. Takeda, K. Hayakawa, A. Matsuzawa, S. Akahane, M. Isaji, and M. Akahane. 2005. Physiological difference between obese (fa/fa) Zucker rats and lean Zucker rats concerning adiponectin. *Metabolism.* **54:** 995–1001.
34. Gibbons, G. F., D. Wiggins, A. M. Brown, and A. M. Hebbachi. 2004. Synthesis and function of hepatic very-low-density lipoprotein. *Biochem. Soc. Trans.* **32:** 59–64.
35. Donnelly, K. L., C. I. Smith, S. J. Schwarzenberg, J. Jessurun, M. D. Boldt, and E. J. Parks. 2005. Sources of fatty acids stored in liver and secreted via lipoproteins in patients with nonalcoholic fatty liver disease. *J. Clin. Invest.* **115:** 1343–1351.
36. Youssef, W. I., and A. J. McCullough. 2002. Steatohepatitis in obese individuals. *Best Pract. Res. Clin. Gastroenterol.* **16:** 733–747.
37. Hussain, M. M., P. Rava, X. Pan, K. Dai, S. K. Dougan, J. Iqbal, F. Lazare, and I. Khatun. 2008. Microsomal triglyceride transfer protein in plasma and cellular lipid metabolism. *Curr. Opin. Lipidol.* **19:** 277–284.
38. García-Ruiz, I., C. Rodríguez-Juán, T. Díaz-Sanjuan, M. A. Martínez, T. Muñoz-Yagüe, and J. A. Solís-Herruzo. 2007. Effects of rosiglitazone on the liver histology and mitochondrial function in ob/ob mice. *Hepatology.* **46:** 414–423.
39. Koo, H. Y., M. A. Wallig, B. H. Chung, T. Y. Nara, B. H. S. Cho, and M. T. Nakamura. 2008. Dietary fructose induces a wide range of genes with distinct shift in carbohydrate and lipid metabolism in fed and fasted rat liver. *Biochim. Biophys. Acta.* **1782:** 341–348.
40. Butterworth, R. F. 2000. Complications of cirrhosis III. Hepatic encephalopathy. *J. Hepatol.* **32:** 171–180.

41. Miyazaki, M., H. Sampath, X. Liu, M. T. Flowers, K. Chu, A. Dobrzyn, and J. Ntambi. 2009. Stearoyl-CoA desaturase-1 deficiency attenuates obesity and insulin resistance in leptin-resistant obese mice. *Biochem. Biophys. Res. Commun.* **380:** 818–822.
42. Grattagliano, I., V. O. Palmieri, P. Portincasa, A. Moschetta, and G. Palasciano. 2008. Oxidative stress-induced risk factors associated with the metabolic syndrome: a unifying hypothesis. *J. Nutr. Biochem.* **19:** 491–504.
43. Rubio, A., E. Guruceaga, M. Vazquez-Chantada, J. Sandoval, L. A. Martínez-Cruz, V. Segura, J. L. Sevilla, A. Podhorski, F. J. Corrales, L. Torres, et al. 2007. Gene-pathway identification associated with non-alcoholic steatohepatitis. *J. Hepatol.* **46:** 708–718.